# Development of a Novel Virtual Screening Cascade Protocol to Identify Potential Trypanothione Reductase Inhibitors

Rolando Perez-Pineiro,*[,†] Asdrubal Burgos,[†] Deuan C. Jones,[‡] Lena C. Andrew,[▽] Hortensia Rodriguez,[§] Margarita Suarez,[§] Alan H. Fairlamb,[‡] and David S. Wishart*[,†]

*Department of Biological Sciences and Computing Science, University of Alberta, Edmonton, Alberta, Canada T6G 2E8, Division of Biological Chemistry & Drug Discovery, College of Life Sciences, University of Dundee, Dundee DD1 5EH, United Kingdom, Laboratorio de Síntesis Orgánica, Facultad de Química, Universidad de la Habana, 10400 Ciudad Habana, Cuba*

*Received October 16, 2008*

The implementation of a novel sequential computational approach that can be used effectively for virtual screening and identification of prospective ligands that bind to trypanothione reductase (TryR) is reported. The multistep strategy combines a ligand-based virtual screening for building an enriched library of small molecules with a docking protocol (AutoDock, X-Score) for screening against the TryR target. Compounds were ranked by an exhaustive conformational consensus scoring approach that employs a rank-by-rank strategy by combining both scoring functions. Analysis of the predicted ligand−protein interactions highlights the role of bulky quaternary amine moieties for binding affinity. The scaffold hopping (SHOP) process derived from this computational approach allowed the identification of several chemotypes, not previously reported as antiprotozoal agents, which includes dibenzothiepine, dibenzooxathiepine, dibenzodithiepine, and polycyclic cationic structures like thiaazatetracyclo-nonadeca-hexaen-3-ium. Assays measuring the inhibiting effect of these compounds on *T. cruzi* and *T. brucei* TryR confirm their potential for further rational optimization.

## Introduction

Trypanosomatids are parasitic protozoa responsible for several tropical diseases of which African sleeping sickness (*Trypanosoma brucei gambiense and T. b. rhodesiense*), Chagas disease (*T. cruzi*), and the different forms of leishmaniasis (*Leishmania donovani and L. infantum*) are considered the most lethal.[1] At present, the chemotherapies associated with all forms of trypanosomiasis have many deficiencies including poor efficacy, toxicity to humans, high cost, and the emergence of drug-resistant parasitic strains.[2] Unfortunately, because of the low profit margins associated with developing improved therapies for tropical diseases, there is little motivation for the pharmaceutical industry to develop better tropical disease drugs. Accordingly, many agencies, including the Special Program for Research and Training in Tropical Diseases at the World Health Organization (WHO/TDR), numerous academic research groups, various international/national bodies, and philanthropic foundations, have been supporting the discovery of new drug candidates for a number of tropical diseases.[3]

One of the most promising strategies to develop potent and specific antiparasitic drugs relies on the exploitation of metabolic differences between the pathogen and the host. The mammalian redox defense system, based on the glutathione/glutathione reductase (GR[a]) couple, is replaced in trypanosomatids by an analogous, but distinct, system based on the thiol−polyamine conjugate trypanothione and the flavoenzyme trypanothione reductase[4] (Figure 1). The almost total mutual substrate exclusivity of these two enzymes and the essential role of TryR in the survival of all trypanosomatids studied so far have served as the basis for rational design of many types of selective inhibitors of TryR in the presence of host GR.[5,6]

Structure-based drug design[7] (SBDD) has emerged as a very effective and low-cost strategy to improve the rate of success at any stage of the drug discovery pipeline. There are two broad categories of SBDD computational techniques: (1) protein−ligand docking and (2) ligand similarity methods. Protein−ligand docking attempts to use the 3D protein structure of the protein target to predict binding modes and affinities of ligands to biologically relevant targets, while ligand-similarity methods capitalize on the fact that ligands similar to an active ligand are more likely to be active than random ligands. The latter method considers two- or three-dimensional chemistry, shape, electrostatic, and interaction points (e.g., pharmacophore points) to assess similarity.

The discovery and optimization of antiparasitic compounds has also profited from the use of computational docking techniques.[8] The elucidation of the 3D structure of TryR in free form[9−11] and complexed with NADPH,[11] glutathionylspermidine,[12] trypanothione,[13] the competitive inhibitor quinacrine[14] and its alkylating derivative quinacrine mustard,[15] have all provided detailed information about the interactions involved in enzyme recognition and substrate binding. Despite this, TryR has been the target of just a few computational approaches and only modest results have been obtained so far. For instance

* To whom correspondence should be addressed. For R.P-P.: phone, 1 780 492 8574; fax, 1 780 492 9234; e-mail: perezpin@ualberta.ca. Address: Department of Biological Sciences, M-330, Biological Sciences Building, University of Alberta, Edmonton, AB Canada T6G 2E9. For D.S.W.: phone, 1 780 492 0383; fax, 1 780 492 1071; e-mail, david.wishart@ualberta.ca.

† Department of Biological Sciences and Computing Science, University of Alberta.

‡ Division of Biological Chemistry & Drug Discovery, College of Life Sciences, University of Dundee.

▽ Present Address: Faculty of Pharmacy and Pharmaceutical Sciences, University of Alberta, Edmonton, Alberta, Canada T6G 2N8.

§ Laboratorio de Síntesis Orgánica, Facultad de Química, Universidad de la Habana.

[a] Abbreviations: TryR, trypanothione reductase; GR, glutathione reductase; SBDD, structure-based drug design; SHOP, scaffold hopping; MCS, maximum common substructure; Spd, spermidine; CS, consensus scoring; AD, AutoDock; XS, X-Score; $Z'$, screening window coefficient.

10.1021/jm801306g CCC: $40.75 
Published on Web 02/19/2009

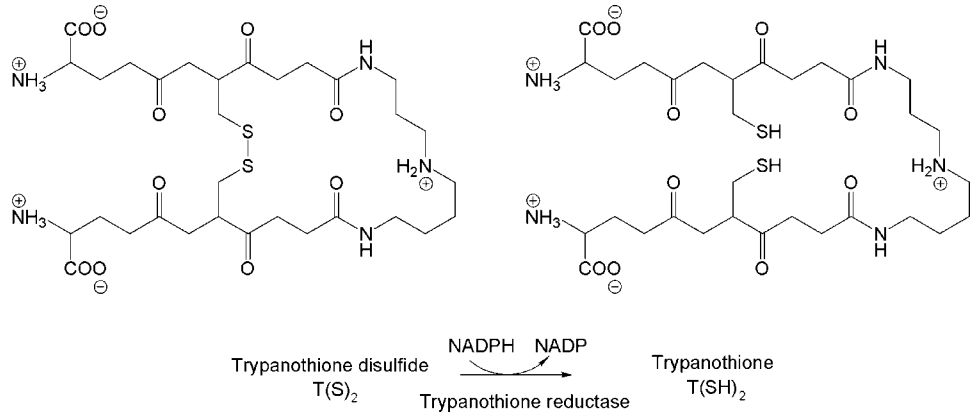


**Figure 1.** Structure of trypanothione ($T(S)_2$) and the reaction catalyzed by trypanothione that reduces $T(S)_2$ to dihydrotrypanothione, $T(SH)_2$.

Horvath's early work employed a rigid-body docking algorithm[16] to predict binding affinity of ligands to TryR. The validity of this docking model is particularly noteworthy in relation to similar computational approaches because it predicted an interaction between the alkyl amino moiety of the acridine ring and the side chain of Glu 19 as observed in the crystal structure of the TryR−quinacrine complex.[14] The discovery of the macrocyclic alkaloid lunarine[13] and the recent identification of chlorhexidine and its derivatives[17] via high-throughput virtual screening are successful examples of the employment of structure-based methodologies to identify novel TryR inhibitors.

At present. trypanothione reductase still poses a tremendous challenge for medicinal chemists. The active site of TryR is extremely wide and it allows for multiple binding orientations and/or the simultaneous accommodation of more than one inhibitor.[15,18,19] In addition, protein−ligand interactions of even very similar compounds can be unpredictable.[20,21] For these reasons, the search for novel structure-based strategies with the ability to identify more potent and selective TryR inhibitors is desirable. In this context, we have decided that the combination of ligand similarity and protein docking strategies in a single workflow could be useful for this purpose. The fact that both methods, when used individually, focus only on one part of the structural information available has recently prompted the development of hybrid similarity-based docking methods. These hybrid methods aim at fully exploiting all the structural information present in ligand-bound protein structures, both from the protein and ligand perspective.[22−24] In principle, a strategy combining 3D ligand similarity and protein docking should provide more accurate prediction about ligand binding modes.[25] Although the majority of ligand similarity-based methods for molecular comparisons, compound classifications, or database searching utilize molecular descriptors for the definition of chemical reference spaces,[26] it has been demonstrated that molecular fragment profiles could also be successfully employed as queries for database searching and that significant recovery rates could be achieved.[27] Fragment profiles differ from molecular fingerprints[28] because, on the one hand, they do not organize predefined or catalogued descriptors in a specific manner, and on the other, they are based on the randomization of structural information rather than canonical bit string representations.

Stemming from our interest in the development of new antiprotozoal drugs,[29] we report herein the first implementation of a novel virtual screening cascade protocol that can be used effectively for virtual screening and identification of prospective ligands that bind to trypanothione reductase. To validate this strategy, we used TryR inhibition assays to measure the activity of 19 of these prospective ligands and we found that many of them exhibit sufficiently promising characteristics to warrant further ligand optimization. The novelty of this approach lies in the sequential combination of a similarity virtual screening based on fragment profile comparisons facilitated through the calculation of compound class-specific fragment frequencies using naive Bayesian statistics, with a docking protocol (AutoDock and X-Score) for screening against the TryR target. Another important feature of this computational approach is the enhancement of its predictive power by incorporating an exhaustive conformational consensus scoring process using a rank-by-rank strategy in order to provide a list of suitable compounds to be considered for bioscreening.

## Computational Methods

The computational approach we developed for screening molecules binding to TryR combines both ligand similarity and protein docking methods within an integrated framework. A flowchart describing various phases of the virtual screening cascade protocol is shown in Figure 2.

**Similarity-Based Virtual Screening.** The Molinspiration virtual screening "miscreen"[30] was selected as the base methodology to perform the ligand-based virtual screening. Briefly, the "miscreen" toolkit first analyses a training set of active structures to build a usable ligand model and then compares it with inactive molecules by using sophisticated Bayesian statistics. On the basis of this analysis, a bioactivity model is developed, where for each substructure fragment a bioactivity contribution is calculated. Once a model is built, the bioactivity of the screened molecules may be then calculated as a sum of the activity contributions of the fragments in these molecules. This approach provides an "activity score" for each compound, which represents the probability that the particular molecule will have the desired biological activity. The higher this score, the higher the probability that the compound will be active.

The construction of the initial training set was based on inhibition mode criteria. Molecules that bind reversibly to trypanothione reductase constitute the largest group of inhibitors studied so far and are among the most effective with inhibition constant ($K_i$) values, usually in the low micromolar range.[5,6] To date, the only reports about the structural determination of TryR complexed with a non-natural substrate are related to the competitive inhibitor quinacrine[14] and its chloro derivative, quinacrine mustard.[15] The availability of these structures certainly provides some useful insights into how these type of ligands fit into the active site of the enzyme and the interactions involved.

In principle, a single active molecule is sufficient to build a usable model, but larger fragment populations have higher

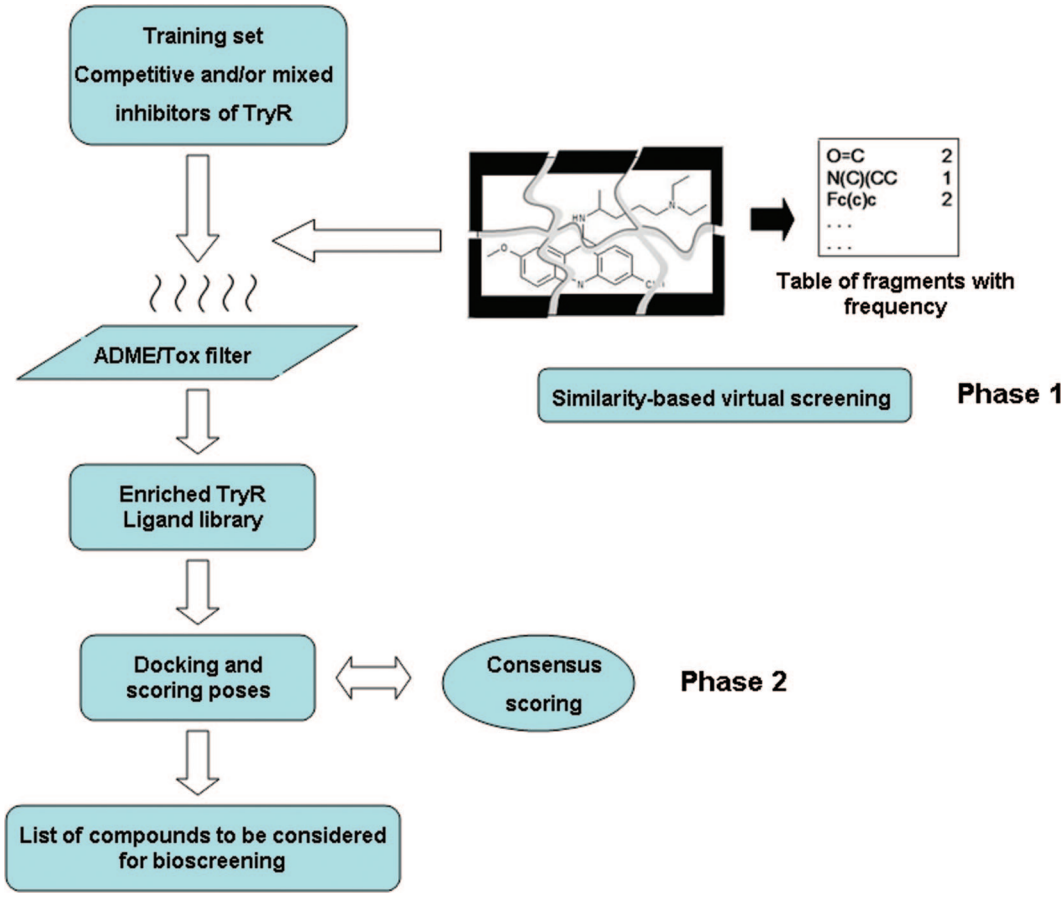


**Figure 2.** Workflow diagram of the virtual screening cascade protocol.

information content, leading to similarity analysis at higher resolution and increasingly accurate compound ranking. The initial training set was assembled using 135 molecules extracted from different bibliographic sources (see Supporting Information) and selected according to their inhibition mode and high binding affinity profiles. Only compounds with $K_i$ values ranging between 0.1−50 $\mu$M were considered. As expected, the majority of the chosen compounds fell into one of the three known general categories of reversible TryR inhibitors: hydrophobic polyamines, tricyclic compounds, and diphenylsulfane derivatives (Figure 3).

Compounds included in the training set were transformed to SMILES coordinates to generate a bioactivity model. The distribution of antiprotozoal activity for 100000 molecules with druglike properties extracted from PubChem by diversity selection to represent the average druglike chemical space and the training set of active structures is shown in Figure 4. According to this diagram, the bioactivity model provides a good separation between active compounds and the average background. Subsequently, in silico screening of the ZINC database (http://zinc.docking.org/), containing over eight million purchasable compounds, was performed by calculating the bioactivity of each molecule as a sum of activity contributions of fragments. A data set of 1312 compounds, listed according to their activity score, typically between 4.3 (higher score) and 1 (lower score), was retrieved.

The "miscreen" virtual screening is very fast (ca. 100000 molecules may be screened in less than an hour) permitting the processing of very large molecular libraries.

**ADME/Tox Filtering.** Filtering of the output data set derived from the similarity-based virtual screening (1312 compounds) was performed by FAF-Drugs[31] (http://bioserv.rpbs.jussieu.fr/Help/FAF Drugs.html). This online service, based on Frowns (a chemoinformatics toolkit), allows users to process their own compound collections via simple ADME/Tox filtering rules such as molecular weight, polar surface area, LogP, or number of rotatable bonds. Notably, FAF-Drugs turned out to be very convenient in our case because its customizable protocol allowed us to input filtering criteria not only related with bioavailability issues but also with substrate specificity. In contrast to GR, the active site of TryR shows an overall negative charge and is much wider and more hydrophobic.[32] Therefore, special attention was given to the input values of total charge (0−$2^+$), LogP (1−5), and molecular mass (200−500). The rest of the parameters were either in compliance with Lipinski's rule of five or set as default. Compounds matching the filtering criteria (603 molecules) comprised the enriched library to be used as input data for docking studies.

**Clustering Analysis of the Enriched Library.** One of the advantages of using a virtual screening protocol based on Bayesian statistics is that it can generalize, i.e., it is able to learn general structure requirements that are necessary for bioactivity. As a result, the newly identified bioactive molecules not only contain building blocks found in the training set. Furthermore, the protocol is also able to identify new chemotypes via a process called scaffold hopping (SHOP). To shed some light about this point, clustering analysis of the initial training set and the enriched library was carried out through LibMCS,[33] a stand-alone application program, part of the JKlustor package. LibraryMCS clusters a set of chemical structures in a hierarchical manner based on the concept of maximum common substructure (MCS). The LibMCS program

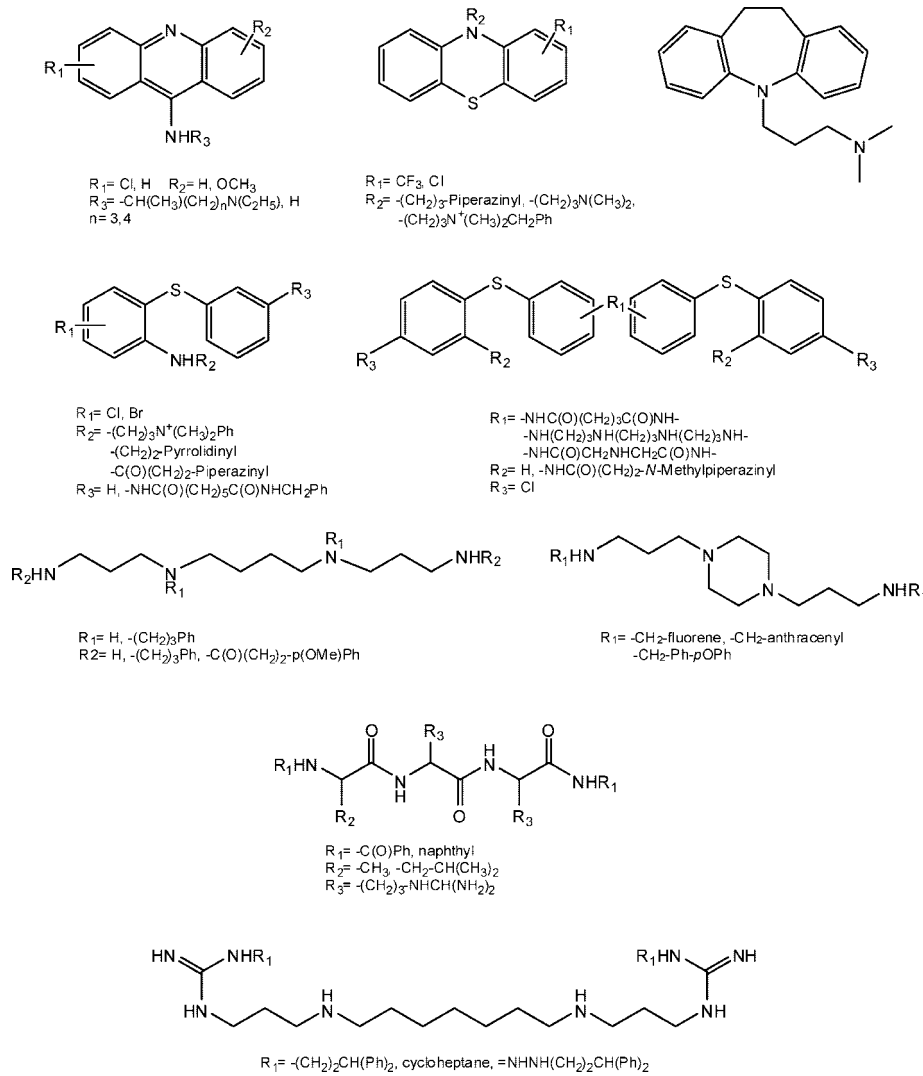


**Figure 3.** General representation of structural templates included in the initial training set.

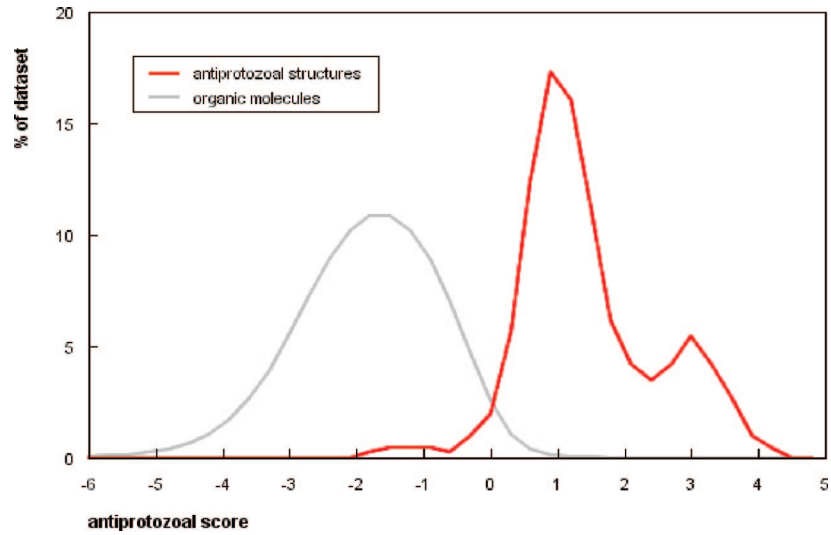


**Figure 4.** Distribution of antiprotozoal activity for average background molecules and the training set based on the bioactivity model.

creates a hierarchical dendrogram representation of the clusters. Structures that share a large common substructure (a core or scaffold structure) are grouped together. In the next step, these cores are clustered to form the next level in the hierarchy. Two hierarchical clusterings, corresponding to the initial training set and the enriched library, respectively, are depicted in Figure 5. Initial structures are found at the bottom of the hierarchy, and the next level contains the MCS of clusters of initial molecules. The highest clustering values observed for the enriched library (cluster level: 4, total cluster count: 257), Figure 5B, with respect

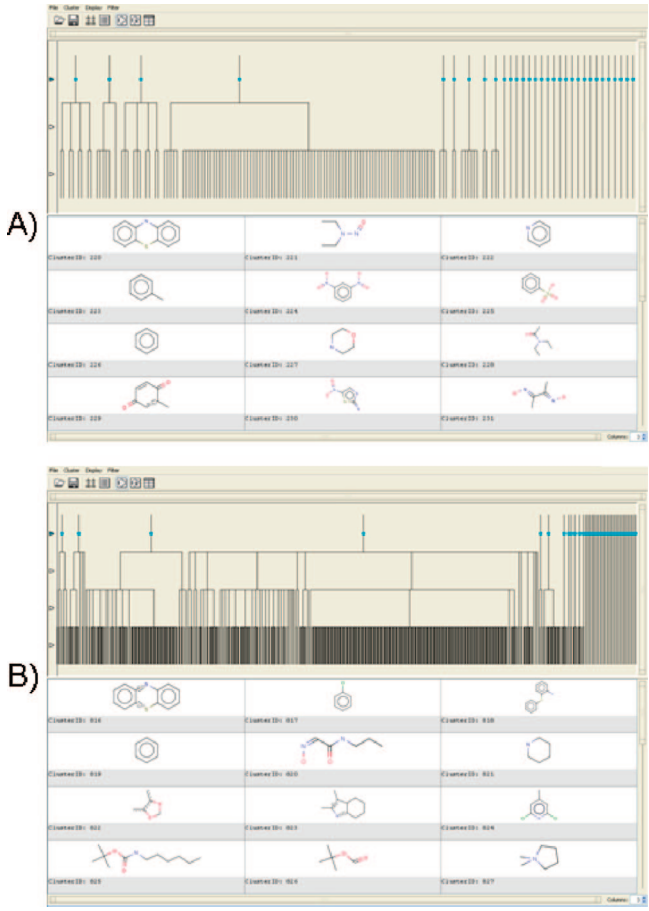


**Figure 5.** Hierarchical clustering dendogram (A) training set, (B) enriched library. Blue rectangle denotes molecules that share the same common structure highlighted in red.

to the initial training set (cluster level: 3, total cluster count: 101), Figure 5A, confirms the effectiveness of the adopted similarity-based strategy to generate new chemotypes by using the information of already known bioactive molecules.

**Docking Studies.** Virtual docking was performed using the Lamarckian genetic algorithm implemented in AutoDock4.[34] This is commonly regarded as best of the three docking methods in AutoDock in terms of its ability to find the lowest energy and its structure prediction accuracy.[35] The protein structure for the unbound *Trypanosoma cruzi* trypanothione reductase was chosen as the target, and coordinates were downloaded from the Protein Data Bank (PDB code 1AOG).[36] Prior to docking, FAD cofactors and water molecules were removed manually from the PDB file. Polar hydrogens were added using the AutoDock Tools interface. Grid maps were prepared using the AutoGrid utility with 126 × 126 × 102 points and grid spacing set to 0.204 Å. Docking parameters modified from the defaults were: number of individuals in the population (set to 300), maximum number of energy evaluations (set to 2500000), maximum number of generations (set to 2700), and number of hybrid GA-LS runs (set to 100).

Initial conformations of the ligands were placed next to the aromatic ring of Tyr111, a central residue in the active site having a hydrophobic interaction with trypanothione. All rotatable bonds in the ligands were allowed to rotate during the docking trials. Because amino acid positions in the enzyme were found, experimentally, to change insignificantly upon binding the native substrate,[12,13] the active site was assumed to be rigid and therefore nonflexible docking was carried out. Ligand structures (603) were taken from version 8.0 of the ZINC Database.[37] For some compounds that were not available in the ZINC Database, sets of coordinates were generated by submitting their SMILE strings to ZINC's user upload utility. In-house Perl scripts were used to extract the 100 conformations generated by AutoDock from the docking output file for each of the compounds in order to allow them to be evaluated by the program X-Score.[38] All ligand files that had the same LogP values calculated by X-Score were inspected visually to verify their structures. Compounds whose files were found to be incorrect had their SMILE strings submitted to ZINC's user upload utility to regenerate their three-dimensional structures and were rescreened. To minimize the computing time, docking jobs as well as X-Score evaluations were carried out on a WestGrid computer cluster designed for serial processing and parallel jobs (http://www.westgrid.ca). Jobs were submitted using portable batch system (PBS) files invoking either AutoDock or X-Score.

In-house Perl scripts were used to extract the top conformations for each compound docked to the protein. Pymol v0.99[39] was used to visualize the compounds docked to the active site of the protein, and schematic diagrams of protein−ligand interactions were obtained by the Ligplot program.[40]

**Consensus Scoring.** Combining multiple scoring functions has been shown in various virtual database screening studies to be an effective way for improving hit rates.[41] While AutoDock is one of the most cited docking programs[42] and has recorded many successes in virtual screening approaches,[43] the standalone scoring function X-Score has shown good correlations between theoretical and experimentally determined protein−ligand binding affinities.[44] Consequently, X-Score was combined in this study with the function implemented in the AutoDock program to provide a list of ligands sorted by consensus scoring adopting the rank-by-rank strategy.[45] AutoDock and X-Score were applied to rank all the conformations generated by the 603 compounds (60300 conformations in total). For each conformation, the final rank was calculated as the average rank from the two scoring functions. Only the best scored conformation of each compound was considered for ranking the 603 ligands.

## Results and Discussion

**Docking Analysis and Enzymatic Assays.** A representation of the 20 top ranked ligands according to consensus scoring is shown in Figure 6. These compounds exhibit structural characteristics typical of several known TryR inhibitors, including extended hydrophobic moieties tethered to positive charge fragments mostly represented by bulky quaternary cyclic amines. The latter feature agrees with the previous finding that positive charges play a crucial role for ligand binding in the active site of TryR.[19,46] Phenothiazines and diphenylsulfanes, included in the initial training set, were successfully recovered among the top scored ligands, highlighting the importance of these building blocks for binding affinity. The presence of a chloro substituent is another common structural motif found in the retrieved molecules. In the TryR−Quinacrine complex, the chlorine atom is close to the ring nitrogen of Trp22. Obviously the halogen is stabilized by interacting with the positively polarized hydrogen of the indolyl nitrogen. The same type of interaction is also very likely to occur for some of the newly identified chloro derivatives.

To test the efficacy of our computational protocol, 19 compounds were screened for inhibition using a high-throughput microplate assay previously developed for this purpose.[47] The

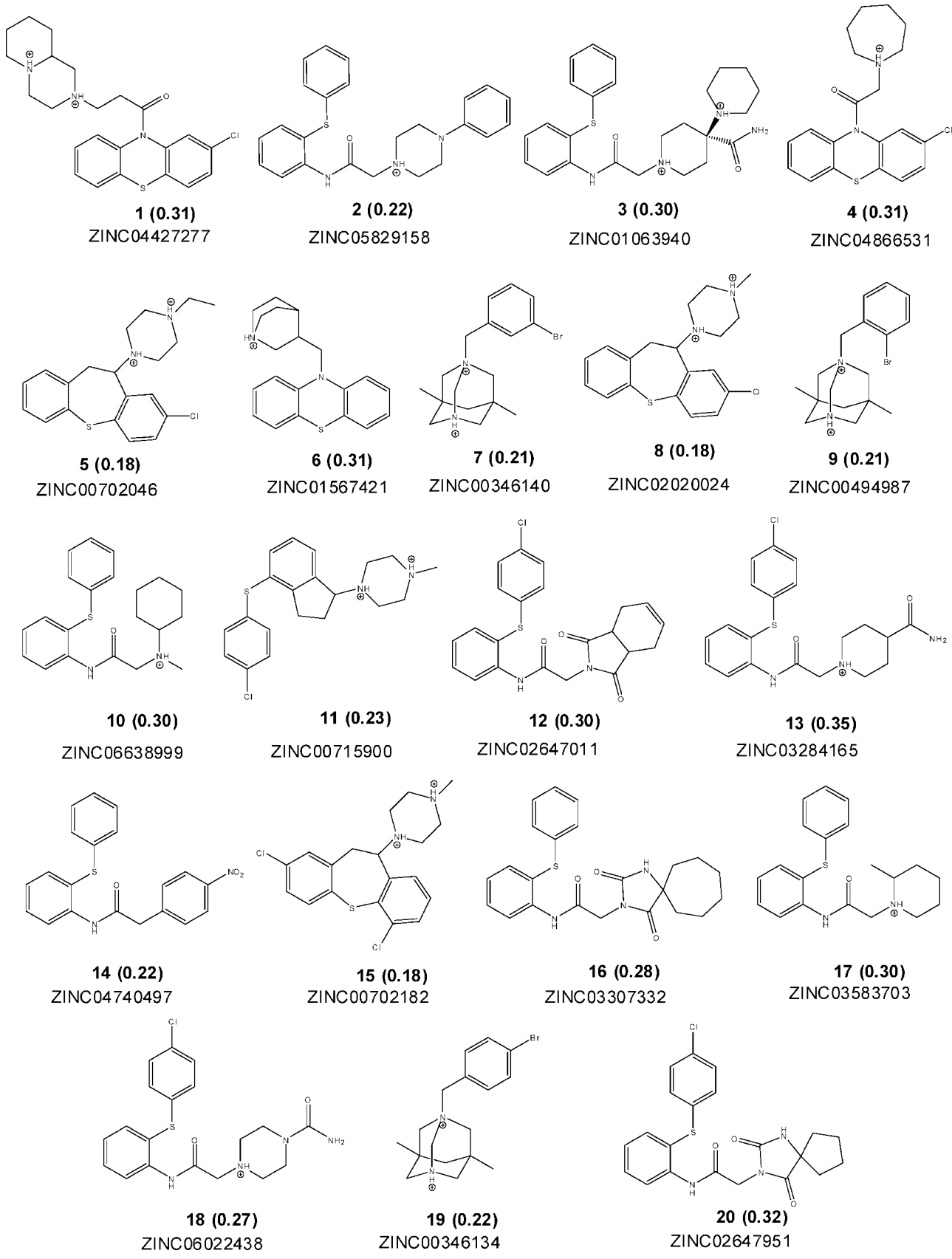


**Figure 6.** Top 20 rank structures from the CS after docking to TryR. Calculated Tanimoto similarity coefficient with respect to quinacrine mustard (in parenthesis).

tested set included 10 of the best rank structures according consensus scoring (compounds **1**−**7**, **10**, **12**, **16**, Figure 6). Additionally, some of the best hits by Autodock (**21**) and X-Score (**22**, **23**, **24**) and several high-ranked new chemotypes (**25**−**29**) depicted in Figure 7, were also considered for screening. Compounds were tested in triplicate against both *T. cruzi* and *T. brucei*. The mean $Z'$ value[48] over the total 19 testing plates was 0.88 (range 0.56−0.96), indicating a well performing

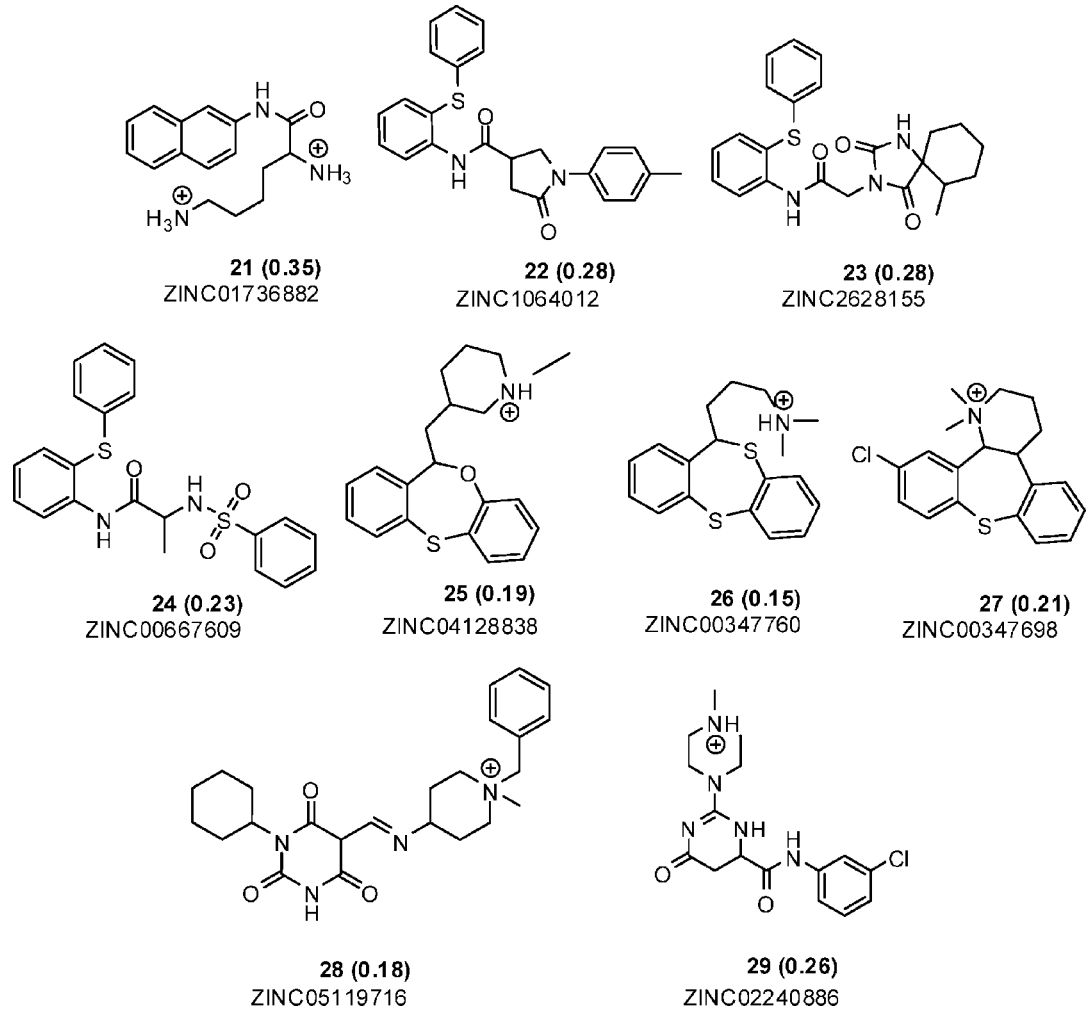


**Figure 7.** Compounds selected from the database for TryR inhibition screening. Calculated Tanimoto similarity coefficient with respect to quinacrine mustard (in parenthesis).

**Table 1.** Inhibition of TryR by Selected Compounds Retrieved from the Virtual Screening Cascade Protocol and their Rankings by Consensus Scoring (CS), AutoDock (AD), and X-Score (XS)

| compd | CS | AD | XS | *T. cruzi* TryR $IC_{50}$ ($\mu$M) | *T. brucei* TryR $IC_{50}$ ($\mu$M) |
|---|---|---|---|---|---|
| **1** | 1 | 4 | 15 | 35.4 ± 1.5 | 31.9 ± 1.4 |
| **2** | 2 | 27 | 2 | >100 | >100 |
| **3** | 3 | 2 | 69 | >100 | >100 |
| **4** | 4 | 28 | 14 | 78.7 ± 8.2 | >100 |
| **5** | 5 | 15 | 76 | 29.1 ± 1.1 | 36.0 ± 1.1 |
| **6** | 6 | 5 | 83 | 21.8 ± 1.2 | 54.3 ± 4.8 |
| **7** | 7 | 49 | 89 | >100 | >100 |
| **10** | 10 | 21 | 58 | 56.3 ± 6.9 | 46.9 ± 6.0 |
| **12** | 12 | 69 | 16 | >100 | >100 |
| **16** | 16 | 83 | 6 | >100 | >100 |
| **21** | 70 | 8 | 259 | >100 | >100 |
| **22** | 112 | 191 | 1 | >100 | >100 |
| **23** | 23 | 46 | 3 | 84.4 ± 4.4 | >100 |
| **24** | 44 | 36 | 4 | >100 | >100 |
| **25** | 26 | 29 | 57 | 11.5 ± 0.4 | 14.6 ± 0.8 |
| **26** | 28 | 68 | 126 | 36.7 ± 2.2 | 37.3 ± 1.1 |
| **27** | 34 | 153 | 77 | 75.3 ± 3.2 | 58.7 ± 2.0 |
| **28** | 27 | 134 | 36 | 45.2 ± 2.8 | >100 |
| **29** | 227 | 105 | 305 | >100 | >100 |

assay. The triplicate $IC_{50}$ values were used to calculate a mean weighted to the standard error, and these values are given in Table 1.

Gratifyingly some of the best hits by consensus scoring (**1**, **5**, **6**, **10**) displayed good inhibitory activity against TryR from both species of parasite, with $IC_{50}$ values ranging between 21−56 $\mu$M. To shed some light about the probable binding modes of these ligands, a computational model of the complex between TryR and the 2-(3-(2-chloro-10*H*-phenothiazin-0-yl)-3-oxopropyl) decahydropyrido[1,2-*a*]pyrazine-2,5-diium (**1**) and 1-(10,11-dihydrodibenzo[*b*,*f*]thiepin-10-yl)-4-ethylpiperazine-1,4-diium (**5**) as well as the protein−ligand interactions involved according to the Ligplot software are depicted in Figure 8. Of particular importance for substrate specificity are five residues in the disulfide substrate binding site that are not conserved when comparing TryR and human GR: Glu19, Trp22, Ser110, Met114, and Ala343. As shown in Figure 8, the low-energy model for both ligands exhibited contacts with several of these key residues in accordance with a pure competitive type of inhibition.

Three possible binding modes were calculated for compound **1** at the active site, Figure 8a. Consensus scoring predicted a very specific hydrogen bond interaction with the oxygen atom of Glu19 side chain and placed the pyridopyrazine-2,5-diium moiety near Trp22, Tyr111, and Leu18. This is the region in TryR that also fixes the spermidine moiety (Spd site) and is thus responsible for the mutually exclusive substrate specificities when comparing the parasite TryR and human GR.[13] In turn. the phenothiazine ring exhibits hydrophobic interactions with Ile339, Pro336. and Asn340. These residues form a pocket that has been reported to accommodate the $\gamma$GluI component of $T[S]_2$,[13] Figure 8b. In contrast to the binding mode predicted

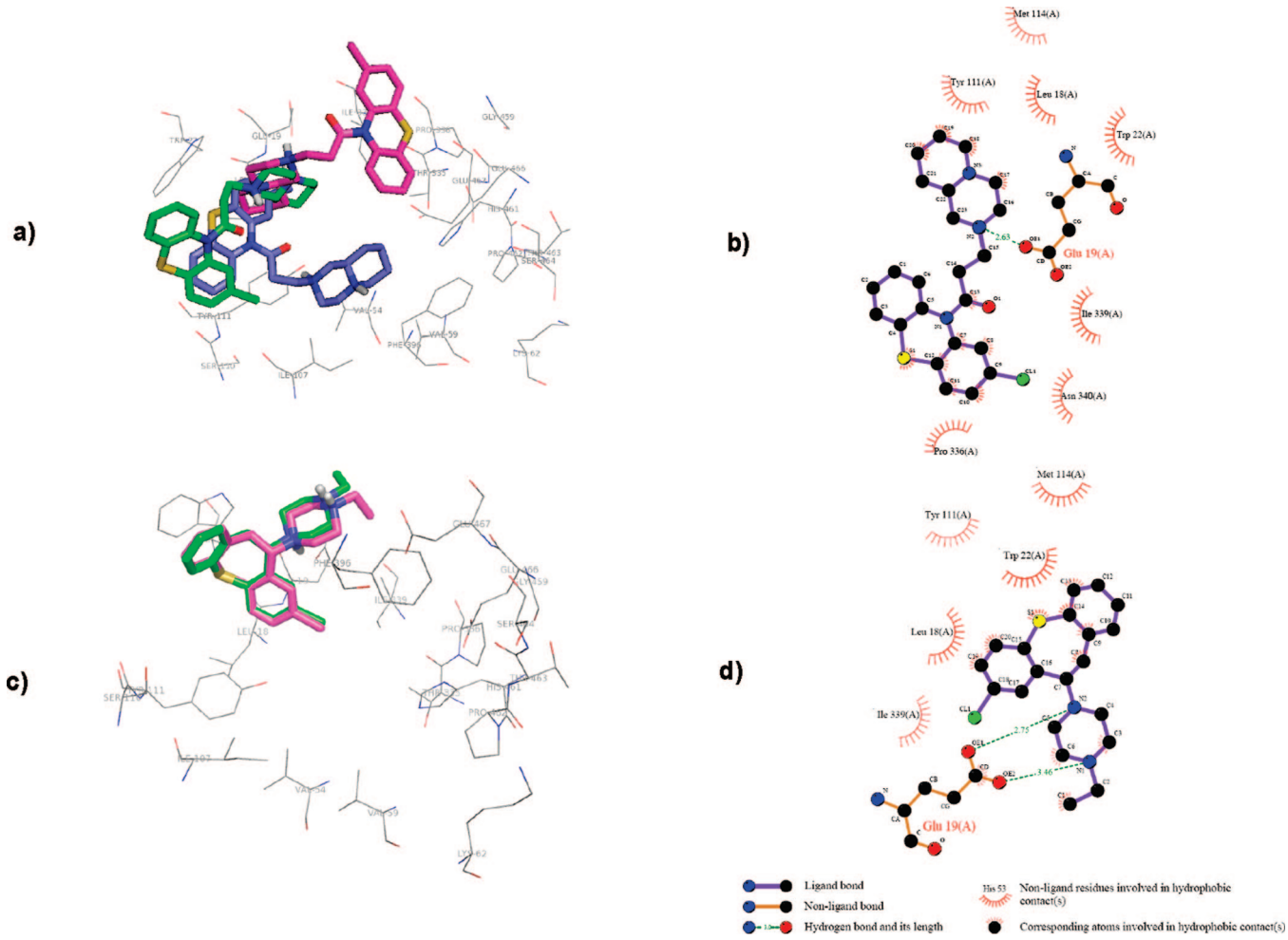


**Figure 8.** View of possible binding modes of protonated compounds **1** (a) and **5** (c) in the active site of TryR predicted by consensus scoring (pink), AutoDock (green), and X-Score (blue). Residues of the active site are shown in atomic colors. Predicted hydrophobic and electrostatic interactions of compounds **1** (b) and **5** (d) at the active site according to Ligplot. Hydrogen bonds and length are represented by dotted lines.

by consensus scoring, the other two calculated conformations positioned the phenothiazine ring near the Spd site and, according to X-Score, the positively charged fragment is at hydrogen bonding distance from Tyr111. On the other hand, two very similar orientations were found for compound **5**, Figure 8c. In both cases, the dithiepine ring is lodged near the Spd site in close contact with residues Trp22, Met114, Leu18, and Tyr11, meanwhile the heavily charged methylpiperazine-1,4-diium moiety displays strong electrostatic interaction with Glu19, Figure 8d.

A similar docking pattern was found for 3-((10*H*-phenothiazin-10-yl)methyl)-1-azoniabicyclo[2.2.2]octane (**6**), and *N*-methyl-*N*-(2-*oxo*-2-(2-(phenylthio)phenylamino) ethyl)cyclohexanaminium (**10**). On the basis of these preliminary docking results, we could assume that the presence of bulky quaternary amines fragments in the analyzed molecules has an important role in enhancing TryR binding affinity. A possible explanation to this fact could be the effective combination of strong electrostatic and hydrophobic interactions between these positively charge moieties and several key residues at the active site that are intimately associated with substrate specificity.

Compounds **2** and **3**, Table 1, showed poor correlation between their theoretical binding affinity and the experimental inhibitory potency. A likely explanation for this fact could be the lack of rigidity in the diphenylsulfide class and the consequent difficulty to accurately predict the energy associated with the ligand−receptor complex.

Compounds **12**, **14**, **16**, and **20** are the only neutral molecules among the 20 top ranked ligands. In contrast to positively charged aromatic compounds, it has been found that neutral species are less likely to induce host toxicity upon DNA binding and they also possess a better availability to cross the blood−brain barrier.[5] The latter property is particularly desirable in the treatment of late-stage parasitic diseases when the parasite have established themselves in the central nervous system.[5] According to the results in Table 1, neither **12** nor **16** displayed significant inhibitory activity against TryR. In the same manner, some of the best ranked ligands by AutoDock (**21**) and X-Score (**22**-**24**) failed to show significant inhibition at concentrations below 100 $\mu$M.

The low values of the Tanimoto similarity coefficient, with respect to the acridine quinacrine mustard, calculated for some of the newly identified chemotypes depicted in Figure 6 and 7 (**7**, 0.21; **5**, 0.18; **11**, 0.23; **25**, 0.19; **26**, 0.15; **27**, 0.21; **28**, 0.18; **29**, 0.26), also confirm the good SHOP performance of the implemented similarity strategy. In this context, the possibility of identifying novel tricyclic-related inhibitors would be of great value because most of the synthetic approaches in this area have been focused toward the decoration of known templates rather than the search for new tricyclic scaffolds.[15,18−20] Gratifyingly, we found that molecules containing dibenzothiepine **5**, dibenzooxathiepine **25**, and dibenzodithiepine **26** heterocycles as a central core could be considered as suitable candidates to increase the limited repertoire of existing tricyclic inhibitors.

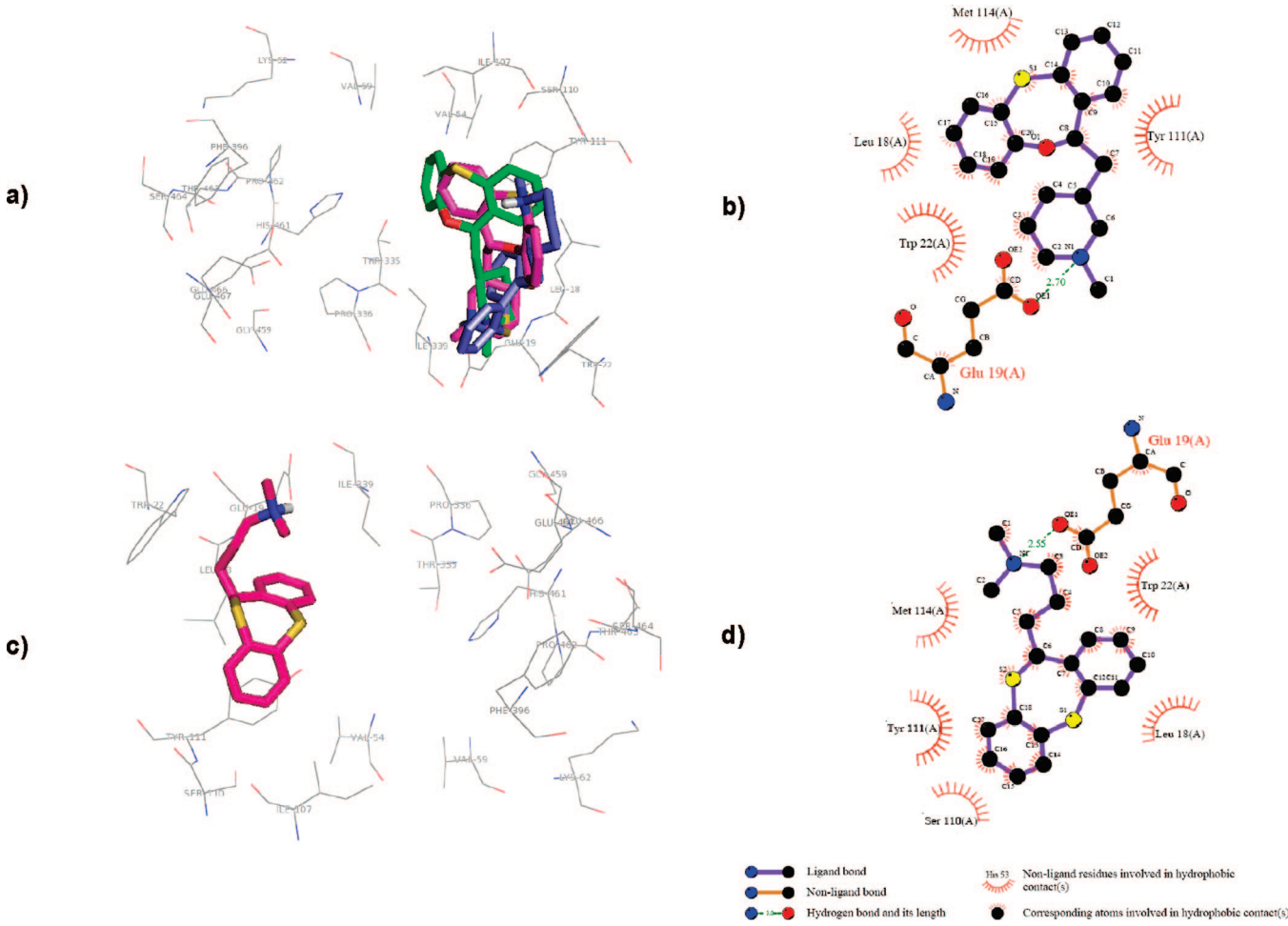


**Figure 9.** View of possible binding modes of compounds **25** (a) and **26** (c) in the active site of TryR predicted by consensus scoring (pink), AutoDock (green) and X-Score (blue). Residues of the active site are shown in atomic colors. Predicted hydrophobic and electrostatic interactions of compounds **25** (b) and **26** (d) at the active site according to Ligplot. Hydrogen bonds and length are represented by dotted lines.

These heterocyclic systems are present in several of the top-ranked molecules, and they have been used as inhibitors of tumor necrosis factor-α,[49] DNA helicases,[50] as well as neurotropic and psychotropic agents.[51]

Moreover, these tricyclic derivatives displayed a good inhibitory activity compound, **25** being the most potent among the tested ligands with $IC_{50}$ values of 11.5 and 14.6 $\mu$M for *T. cruzi* and *T. brucei* TryR, respectively, Table 1. The preferred conformation found for 3-((11*H*-dibenzo[*b*,*e*][1,4]oxathiepin-11-yl)methyl)-1-methylpiperidinium (**25**) and 3-(11*H*-dibenzo[*b*,*e*][1,4]dithiepin-11-yl)-*N*,*N*-dimethylpropan-1-aminium (**26**) at the active cleft, and the ligand−protein interactions involved are depicted in Figure 9. As expected, these compounds display a binding pattern similar to that proposed for the tricyclic inhibitors acridine and phenothiazine. Three modes of binding were found for compound **25**, Figure 9a. Even though all the conformations anchored the tricyclic dibenzooxathiepine in the proximity of the hydrophobic patch (Trp22, Met114, Tyr111, Leu18), only AutoDock and consensus scoring positioned the 1-methylpiperidinium moiety at hydrogen bond distance from Glu19, Figure 9b. A similar orientation was found for **26**, Figure 9c. The bulky dibenzodithiepine moiety is anchored at the Spd site (Trp22, Met114, Ser110), and the alkyl amino side chain exhibits electrostatic interactions with Glu19 via hydrogen bonding, Figure 9d.

The thia-3-azatetracyclo **27** and the 2,4,6-trioxohexahydropyrimidine **28** also constitutes novel chemotypes found among the top rank molecules. Compound **27** possesses moderate inhibitory activity (58−75 $\mu$M), meanwhile **28** shows an unexpected selectivity for inhibiting *T. cruzi* TryR (45 $\mu$M) because little inhibition was detected under 100 $\mu$M for *T. brucei* TryR.

Recently, the importance of terminally substituted guanidines and biguanides for antitrypanosomal activity has been highlighted. The biguanide clorhexidine,[18] and several alkylpolyaminoguanidines and alkylpolyaminobiguanides,[52] have shown potent inhibitory activity against TyrR. Assuming that these derivatives would produce an entropy penalty upon binding, the employment of 4-*oxo*-1,4,5,5-tetrahydropyrimidin-2-yl-piperazin-1-ium **29**, as a conformationally constrained bioisosters of guanidine, seems to be a viable alternative. Nevertheless, this compound failed to show significant inhibition at concentrations below 100 $\mu$M.

## Conclusions

The development of a novel virtual screening cascade protocol to identify potential inhibitors of the parasitic enzyme trypanothione reductase has been described. On the basis of molecular fragment profiles, a similarity search on the ZINC database was performed by the "miscreen" program using known reversible inhibitors of TryR as reference structures. After ADME/TOX filtering, the resulting enriched library was docked into the binding site of TryR to provide a list of putative ligands ranked according to consensus scoring. Clustering analysis and Tan-

imoto values of selected compounds confirms a notable improvement of the molecular diversity of the enriched library with respect to the initial training set. The study of electrostatic and hydrophobic interactions of the best hits at the active cleft highlighted the importance of conformationally constrained quaternary amine moieties in enhancing TryR binding affinity. Enzymatic inhibition assays on *T. cruzi* and *T. brucei* TryR confirmed the inhibitory effect of some of the top ranked ligands. In addition, the scaffold hopping (SHOP) process derived from the developed computational approach allowed the identification of several chemotypes not previously tested as antiprotozoal agents. To our knowledge, this is the first report about the inhibitory effect of molecules-containing dibenzothiepine, dibenzooxathiepine, dibenzodithiepine, thiaazatetracyclo, and 2,4,6-trioxohexahydro pyrimidine on trypanothione reductase. Further rational optimization of these polycyclic ring systems and the bioscreening of the rest of the structures contained in the database are the theme of future research.

## Experimental Section

Compounds used for inhibitory testing were supplied by different commercial sources. Compounds **5** (salt, $CH_3SO_3H$), **24**, **25** (salt, HOOCCOOH), **26** (salt, HOOCCOOH), and **27** (salt, $Cl^-$ $H_2O$) were from SPECS (http:www.specs.net); **3**, **4** (salt, HCl), and **22** were from Chembridge (http:www.chembridge.com); **6**, **7** (salt, $Cl^-$), and **28** (salt, I) were from IBScreen (http:www.ibscreen.com); **2**, **10**, **12**, **16**, **23**, and **29** were from Enamine (http:www.enamine.net); **1** (salt 2 × HOOCCHCHCOOH) was from TimTec (http:www.timtec.net), and **21** (salt $CO_3^{2-}$) was from Bachem.

The purity of the tested compounds was determined by liquid chromatography-MS (Phenomenex Gemini C18 column, 50 mm × 3.0 mm, 5 $\mu$m particle size; mobile phase, water/acetonitrile +0.1% HCOOH 80:20 to 5:95 over 3.5 min and then held for 1.5 min; flow rate 0.5 mL/min). Samples were diluted with acetonitrile/water (1:1) and analyzed using UV detection at 254 nm. According to the analytical data the purity of the tested compounds is higher than 95% except for compound **10** (43%).

**Enzymatic assays.** Inhibition of TryR was carried out in a microplate format as described previously.[45] Assays were set up in 96-well plates using a Biotek Precision 2000 automated liquid handler and initiated using NADPH. The final assay mixtures (0.18 mL) contained TR (20 mU/mL) in the presence of 40 mM Hepes (pH 7.5), 1 mM EDTA, 0.15 mM NADPH, 50 $\mu$M 5,5′-dithiobis(2-nitrobenzoic acid), 6 $\mu$M T[S]2, and inhibitor (100 $\mu$M to 10 nM in 3-fold serial dilutions). The linear rate of thionitrobenzoate ion formation was monitored over 5 min in a Spectramax 340PC plate reader (Molecular Devices) at 412 nm. Raw data was processed using Microsoft Excel. Grafit 5.0 (Erithacus software) was used to fit the data to a three-parameter equation to determine $IC_{50}$ values. $IC_{50}$ determinations were carried out in triplicate for each compound and the mean weighted to standard error calculated.

**Acknowledgment.** AHF was funded by the Wellcome Trust (WT 079838). We thank Dr. Mark Berjanski (University of Alberta) and Dr. Lenin Domínguez (Universidad Nacional Autónoma de México) for helpful comments on this manuscript.

**Supporting Information Available:** Known TryR inhibitors contained in the initial training set. This material is available free of charge via the Internet at http://pubs.acs.org.

## References

(1) Sachs, J. D.; Hotez, P. J. Fighting tropical diseases. *Science* **2006**, *311*, 1521.
(2) Renslo, A. R.; McKerrow, J. H. Drug discovery and development for neglected parasitic diseases. *Nat. Chem. Biol.* **2006**, *2*, 701−710.
(3) Nwaka, S.; Hudson, A. Innovative lead discovery strategies for tropical diseases. *Nat. Rev. Drug Discovery* **2006**, *5*, 941–955.
(4) Fairlamb, A. H.; Blackburn, P.; Ulrich, P.; Chait, B. T.; Cerami, A. Trypanothione: a novel bis(glutathionyl)spermidine cofactor for glutathione reductase in trypanosomatids. *Science* **1985**, *227*, 1485–1487.
(5) Krauth-Siegel, R. L.; Bauer, H.; Schirmer, H. Dithiol proteins as guardians of the intracellular redox milieu in parasites: old and new drugs targets in trypanosomes and malaria-causing plasmodia. *Angew. Chem., Int. Ed.* **2005**, *44*, 690–715.
(6) O'Sullivan, M. C. The battle against trypanosomiasis and leishmaniasis: metal-based and natural product inhibitors of trypanothione reductase. *Curr. Med. Chem.* **2005**, *4*, 355–378.
(7) Lange, G. Structure-based drug design—the use of protein structure in drug discovery. In *Comprehensive Medicinal Chemistry II*, 1st ed.; Triggle, D. J., Taylor, J. B., Eds.; Elsevier, Oxford, 2006; Vol. 4; pp 597−650.
(8) Wolf, K.; Dormeyer, M. Information-based methods in the development of antiparasitic drugs. *Parasitol Res.* **2003**, *90*, S91–S96.
(9) Kuriyan, J.; Kong, X. P.; Krishna, T. S.; Sweet, R. M.; Murgolo, N. J.; Field, H.; Cerami, A.; Henderson, G. B. X-Ray Structure of Trypanothione Reductase from *Crithidia fasciculata* at 2.4 Å Resolution. *Proc. Natl. Acad. Sci. U.S.A.* **1991**, *88*, 8764–8768.
(10) Hunter, W. N.; Bailey, S.; Habash, J.; Harrop, S. J.; Helliwel, J. R.; Aboagye-Kwarteng, T.; Smith, K.; Fairlamb, A. H. Active site of trypanothione reductase: A target for rational drug design. *J. Mol. Biol.* **1992**, *227*, 322–333.
(11) Lantwin, C. B.; Schlichting, I.; Kabsch, W.; Pai, E. F.; Krauth-Siegel, R. L. The structure of *Trypanosoma cruzi* trypanothione reductase in the oxidized and NADPH reduced state. *Proteins* **1994**, *18*, 161–173.
(12) Bailey, S.; Smith, K.; Fairlamb, A. H.; Hunter, W. N. Substrate interactions between trypanothione reductase and W-glutathionylspermidine disulphide at 0.28 nm resolution. *Eur. J. Biochem.* **1993**, *213*, 67–75.
(13) Bond, C. S.; Zhang, Y.; Berriman, M.; Cunningham, M. L.; Fairlamb, A. H.; William, N. H. Crystal structure of *Trypanosoma cruzi* trypanothione reductase in complex with trypanothione, and the structure-based discovery of new natural product inhibitors. *Structure* **1999**, *7*, 81–89.
(14) Jacoby, E. M.; Schlichting, I.; Lantwin, C. B.; Kabsch, W.; Krauth-Siegel, R. L. Crystal structure of the *Trypanosoma cruzi* trypanothione reductase·mepacrine complex. *Proteins* **1996**, *24*, 73–80.
(15) Saravanamuthu, A.; Vickers, T. J.; Bond, C. S.; Peterson, M. R.; Hunter, W. N.; Fairlamb, A. H. Two interacting binding sites for quinacrine derivatives in the active site of trypanothione reductase: A template for drug design. *J. Biol. Chem.* **2004**, *279*, 29493–29500.
(16) Horvath, D. A virtual screening approach applied to the search for trypanothione reductase inhibitors. *J. Med. Chem.* **1997**, *40*, 2412–2423.
(17) Meiering, S.; Inhoff, O.; Mies, J.; Vincek, A.; Garcia, G.; Kramer, B.; Dormeyer, M.; Krauth-Siegel, R. L. Inhibitors of *Trypanosoma cruzi* trypanothione reductase revealed by virtual screening and parallel synthesis. *J. Med. Chem.* **2005**, *48*, 4793–802.
(18) Garforth, J.; Yin, H.; McKie, J. H.; Douglas, K. T.; Fairlamb, A. H. Rational design of selective ligands for trypanothione reductase from *Trypanosoma cruzi*. Structural effects on the inhibition by dibenzazepines based on imipramine. *J. Enzyme Inhib.* **1997**, *12*, 161–173.
(19) Khan, M. O.; Austin, S. E.; Chan, C.; Yin, H.; Marks, D.; Vaghjiani, S. N.; Kendrick, H.; Yardley, V.; Croft, S. L.; Douglas, K. T. Use of an additional hydrophobic binding site, the Z site, in the rational drug design of a new class of stronger trypanothione reductase inhibitor, quaternary alkylammonium phenothiazines. *J. Med. Chem.* **2000**, *43*, 3148–3156.
(20) Bonse, S.; Santelli-Rouvier, C.; Barbe, J.; Krauth-Siegel, R. L. Inhibition of *Trypanosoma cruzi* trypanothione reductase by acridines: Kinetic studies and structure−activity relationships. *J. Med. Chem.* **1999**, *42*, 5448–5454.
(21) Ponasik, J. A.; Strickland, C.; Faerman, C.; Savvides, S.; Karplus, P. A.; Ganem, B. Kukoamine A and other hydrophobic acylpolyamines: potent and selective inhibitors of *Crithidia fasciculata* trypanothione reductase. *Biochem. J.* **1995**, *311*, 371–375.
(22) Fradera, X.; Knegtel, M. A.; Mestres, J. Similarity-driven flexible ligand docking. *Proteins* **2000**, *40*, 623–626.
(23) Wu, G.; Vieth, M. SDOCKER: A method utilizing existing X-ray structures to improve docking accuracy. *J. Med. Chem.* **2004**, *47*, 3142–3148.
(24) Kortagere, S.; Welsh, W. J. Development and application of hybrid structure based method for efficient screening of ligands binding to G-protein coupled receptors. *J. Comput.-Aided Mol. Des.* **2006**, *20*, 789–802.
(25) Marialke, J.; Tietze, S.; Apostolakis, J. Similarity Based Docking. *J. Chem. Inf. Model.* **2008**, *48*, 186–196.
(26) Bajorath, J. Selected concepts and investigations in compound classification, molecular descriptors analysis, and virtual screening. *J. Chem. Inf. Comput. Sci.* **2001**, *41*, 233–245.

(27) Batista, J.; Bajorath, J. Chemical database mining through entropy-based molecular similarity assessment of randomly generated structural fragment populations. *J. Chem. Inf. Comput. Sci.* **2007**, *47*, 59–68.
(28) Bajorath, J. Integration of virtual and high-throughput screening. *Nat. Rev. Drug Discovery* **2002**, *1*, 882–894.
(29) (a) Monzote, L.; Montalvo, A. M.; Fonseca, L.; Pérez, R.; Suárez, M.; Rodríguez, H. In vitro activities of thiadiazine derivatives against *Leishmania amazonensis*. *Arzneim. Forschung./Drug Res.* **2005**, *55*, 232–238. (b) Coro, J.; Atherton, R.; Little, S.; Wharton, H.; Yardley, V.; Alvarez, A, Jr.; Suárez, M; Pérez, R.; Rodríguez, H. Alkyl-linked bis-THTT derivatives as potent in vitro trypanocidal agents. *Bioorg. Med. Chem. Lett.* **2006**, *16*, 1312–1315.
(30) Miscreen—Molinspiration Fragment-based Virtual Screening Engine written in Java; http://www.molinspiration.com/docu/miscreen/index.html. Accessed February 15, 2007.
(31) Miteva, M. A.; Violas, S.; Montes, M.; Gomez, D.; Tuffery, P.; Villoutreix, B. O. FAF-Drugs: free ADME/tox filtering of compound collections. *Nucleic Acids Res.* **2006**, *34*, W738−W744.
(32) Faerman, C. H.; Sawides, S. N.; Strickland, C.; Breidenbach, M. A.; Ponasik, J. A.; Ganem, B.; Ripoll, D.; Krauth-Siegel, R. L.; Karplus, P. A. Charge is the major discriminating factor for glutathione reductase versus trypanothione reductase inhibitors. *Bioorg. Med. Chem.* **1996**, *4*, 1247–1253.
(33) Chemaxon; http://www.chemaxon.com. Accessed December 14, 2007.
(34) Huey, R.; Morris, G. M.; Olson, A. J.; Goodsell, D. S. A Semiempirical Free Energy Force Field with Charge-Based Desolvation. *J. Comput. Chem.* **2007**, *28*, 1145–1152.
(35) Morris, G. M.; Goodsell, D. S.; Halliday, R. S.; Huey, R.; Hart, W. E.; Belew, R. K.; Olson, A. J. Automated Docking Using a Lamarckian Genetic Algorithm and an Empirical Binding Free Energy Function. *J. Comput. Chem.* **1998**, *19*, 1639–1662.
(36) Zhang, Y.; Bond, C. S.; Bailey, S.; Cunningham, M. L.; Fairlamb, A. H.; Hunter, W. N. The crystal structure of trypanothione reductase from the human pathogen *Trypanosoma cruzi* at 2.3 A resolution. *Protein Sci.* **1996**, *5*, 52–61.
(37) Irwin, J. J.; Shoichet, B. K. ZINC—A Free Database of Commercially Available Compounds for Virtual Screening. *J. Chem. Inf. Model.* **2005**, *45*, 177–182.
(38) Wang, R.; Lai, L.; Wang, S. Further development and validation of empirical scoring functions for structure-based binding affinity prediction. *J. Comput.-Aided Mol. Des.* **2002**, *16*, 11–26.
(39) DeLano, W. L. The PyMOL Molecular Graphics System, DeLano Scientific: Palo Alto, CA, 2002; http://www.pymol.org.
(40) Wallace, A. C.; Laskowski, R. A.; Thornton, J. M. LIGPLOT: a program to generate schematic diagrams of protein−ligand interactions. *Protein Eng.* **1995**, *8*, 127–134.
(41) Yang, J. M.; Chen, Y. F.; Shen, T. W.; Kristal, B. S.; Hsu, D. F. Consensus scoring criteria for improving enrichment in virtual screening. *J. Chem. Inf. Model.* **2005**, *45*, 1134–1146.
(42) Cummings, M. D.; Desjarlais, R. L.; Gibbs, A. C.; Mohan, V.; Jaeger, E. P. Comparison of automated docking programs as virtual screening tools. *J. Med. Chem.* **2005**, *48*, 962–976.
(43) Lindstrom, W.; Morris, G. M.; Weber, C.; Huey, R. *Using AutoDock for virtual screening*; The Scripps Research Institute Molecular Graphics Laboratory: La Jolla, CA, 2006; pp 1−36.
(44) Wang, R.; Lu, Y.; Wang, S. Comparative Evaluation of 11 Scoring Functions for Molecular Docking. *J. Med. Chem.* **2003**, *46*, 2287–2303.
(45) Wang, R.; Wang, S. How does consensus scoring work for virtual library screening? An idealized computer experiment. *J. Chem. Inf. Comput. Sci.* **2001**, *41*, 1422–1426.
(46) Parveen, S.; Khan, M. O. F.; Austin, S. E.; Croft, S. L.; Yardley, V.; Rock, P.; Douglas, K. T. Antitrypanosomal, antileishmanial, and antimalarial activities of quaternary arylalkylammonium 2-amino-4-chlorophenyl sulfides, a new class of trypanothione reductase inhibitor, and of *N*-acylderivatives of 2-amino-4-chlorophenyl phenyl sulfide. *J. Med. Chem.* **2005**, *48*, 8087–8097.
(47) Hamilton, C. J.; Saravanamuthu, A.; Egglestone, I. M.; Fairlamb, A. H. Ellman's-reagent-mediated regeneration of trypanothione in situ: substrate-economical microplate and time-dependent inhibition assays for trypanothione reductase. *Biochem. J.* **2003**, *369*, 529–537.
(48) Zhang, J.-H.; Chung, T. D. Y.; Oldenburg, K. R. A simple statistical parameter for use in evaluation and validation of high throughput screening assays. *J. Biomol. Screen* **1999**, *4*, 67–73.
(49) Lal, B.; Sharma, S.; Ghosh, U.; Bal-Tembe, S.; More, T.; Gagare, P.; Jadhav, S.; Patil, S.; Kulkarni-Almeida, A.; Parikh, S.; Panicker, R.; Damre, A.; Gupte, R. Fused tricyclic compounds as inhibitors of tumor necrosis factor-α, their preparation, pharmaceutical compositions, and use in therapy. PCT Int. Appl. WO 2006051477, 2006; p 115.
(50) Dubaele, S.; Jahnke, W.; Schoepfer, J.; Fuchs, J.; Chene, P. Inhibition of DNA helicases with DNA-competitive inhibitors. *Bioorg. Med. Chem. Lett.* **2006**, *16*, 923–927.
(51) Sindelar, K.; Holubek, J.; Ryska, M.; Svatek, E.; Dlabac, A.; Hrubantova, M.; Protiva, M. Neurotropic and psychotropic agents. CLXI. Tricyclic psychotropic agents containing two chalcogen atoms in the central ring: synthesis of 11-(dimethylaminoalkyl) derivatives of 11*H*-dibenzo[*b*,*e*]-1,4-dioxepin and 11*H*-dibenzo[*b*,*e*]-1,4-dithiepin. *Collect. Czech. Chem. Commun.* **1982**, *47*, 72–87.
(52) Bi, X.; Lopez, C.; Bacchi, C. J.; Rattendi, D.; Woster, P. M. Novel alkylpolyaminoguanidines and alkylpolyaminobiguanides with potent antitrypanosomal activity. *Bioorg. Med. Chem. Lett.* **2006**, *16*, 3229–3232.

JM801306G